World Journal of Engineering and Technology, 2026, 14(3), 662-683
https://www.scirp.org/journal/wjet
ISSN Online: 2331-4249
ISSN Print: 2331-4222

Numerical Study of Vehicle-Induced Vibrations on the Reinforced Concrete Retaining Wall in Dschang

Edmond Dawak Fezeu[1,2*], Marcelline Blanche Manjia[1,2], Chérif Bishweka Biryondeke[1,3], Élodie Rufine Zang[1,2], Chrispin Pettang[1,2]

[1]Laboratory Engineering Civil and Mechanics, Doctoral Research Unit for Engineering and Applications, University of Yaoundé I, Yaoundé, Cameroon
[2]Department of Civil Engineering, National Advanced School of Engineering, University of Yaoundé I, Yaoundé, Cameroon
[3]Department of Civil Engineering, Free University of the Great Lakes Countries, Goma, Democratic Republic of the Congo
Email: *edmonddawakfezeu@gmail.com

How to cite this paper: Dawak Fezeu, E., Manjia, M.B., Bishweka Biryondeke, C., Zang, É.R. and Pettang, C. (2026) Numerical Study of Vehicle-Induced Vibrations on the Reinforced Concrete Retaining Wall in Dschang. *World Journal of Engineering and Technology*, **14**, 662-683.
https://doi.org/10.4236/wjet.2026.143042

Received: June 18, 2026
Accepted: August 24, 2026
Published: August 27, 2026

Abstract

Reinforced concrete retaining walls located near road infrastructure are subjected to dynamic stresses caused by passing vehicles, generating inertial forces that affect the stresses, displacements, and stability of the structure. In Dschang, where these structures are widely used on uneven terrain, these dynamic loads—which are often more demanding than conventional static assumptions—call traditional design methods into question. Numerical modeling using the finite element method makes it possible to analyze their actual influence on the behavior of these structures. This study aims to evaluate, through finite element numerical modeling, the influence of vibrations induced by road traffic on the dynamic behavior of reinforced concrete retaining walls in the city of Dschang (Cameroon). The goal is to analyze the effects of moving loads on the stresses, deformations, displacements, and overall stability of these structures, in order to highlight the limitations of purely static approaches and emphasize the need to incorporate dynamic loads into their design. The methodology adopted is based on a numerical approach based on previous work carried out in Cameroon. It consists of developing a finite element method model using the SAP2000 software, in order to analyze the dynamic response of the reinforced concrete retaining wall subjected to road loads. This simulation makes it possible to assess the influence of traffic-induced vibrations on the stresses, deformations, displacements, and overall stability of the structure in the specific context of Dschang-Falaise. The results of the study highlight significant differences between the analyses under static loads and under traffic loads. The observed differences in maximum deformations are around 6.40%, 6.16%, and 0.89%, while those related to maximum stresses reach 4.60%, 4.22% and 4.01%. These variations reflect the significant influence of the dynamic effects induced by road traffic on the mechanical response of the reinforced concrete retaining wall. The results obtained highlight the need to integrate traffic loads in the design of reinforced concrete retaining walls, due to their significant influence on the structural response. Furthermore, the analysis of the spectral acceleration response shows a decreasing trend in road traffic-induced overload, indicating that the intensity of the dynamic effect decreases with increasing geometric parameters of the wall. Thus, the dimensions of the structure help to mitigate the impact of dynamic loads related to traffic.

Keywords

Reinforced Concrete Retaining Wall, Structural Analysis, Mobile Load, Traffic Loads, Finite Element Methods (SAP2000), Spectral Acceleration Response

1. Introduction

The Santchou road (Falaise Dschang) has a steep gradient, making it dangerous and accident-prone. The lack of ancillary structures is a major problem on this steep road. These structures contribute to user safety, road durability, and environmental protection. They stabilize steep slopes and prevent landslides, which are common in this mountainous area. The construction of retaining walls is therefore an absolute necessity to guarantee the safety of road users and the durability of the road.

To guarantee its effectiveness, the retaining wall must be designed taking into account the loads due to road traffic. Reinforced concrete retaining walls behave somewhat differently from, but more advantageously than, weight walls in the face of loads from goods vehicles, as there is an interaction between the reinforced concrete part and the backfill. Reinforced concrete walls are among the most commonly used retaining structures, especially in their simplest L-or inverted T-shapes for heights of less than 6 m. They are ideally suited to the construction of embankment structures on land out of water. Reinforced concrete walls are structurally rigid structures.

Reinforced concrete retaining walls over 5.6 m high are complex structures whose behavior is simulated using the FEM elasto-plastic analysis model applied to a three-dimensional model [1] [2]. Their modeling for structural analysis requires the use of various software packages, but very few of them can be modulated with unrealistic fixed assumptions [3]. It is of particular interest to design a digital model that is interactive, scalable, collaborative, more accessible, and capable of adapting to all phases of construction.

However, research by Liu *et al.* (2021) reveals that vehicle position influences horizontal displacement and lateral pressure on the wall [4]. Wang *et al.* (2014)

show that geogrid reinforcement significantly improves the dynamic response of the retaining wall under vehicle loading, reducing dynamic deformations and stresses [5]. Liu *et al.* (2017) present that the lateral soil pressure of the reinforced body is much greater than the lateral soil pressure behind the facing wall [6]. For Ze *et al.* (2019), variable-section walls may have insufficient shear strength in the central and upper parts, leading to shear failures [7]. Sahibbi *et al.* (2024) conclude that the distribution of lateral soil pressure decreases with wall height, and the effect of top surcharge quickly fades. Under dynamic loading, maximum displacement and the risk of sliding increase considerably, while differential settlement decreases with wall height and increases with load intensity [8].

The overall objective of this work is to contribute to current knowledge on the study of the stability of reinforced concrete retaining walls subjected to traffic loads in order to analyze their impact using the finite element method (FEM). The aim is to:

- Prove the limitations of the static calculation method;
- Present the spectral response of road loads;
- Assess the impact of dynamic analysis on design and dimensioning.

In the present work, we are interested in modeling the behavior of external pressure generated by road traffic loads on a reinforced concrete retaining wall that varies at Dschang-Falaise. Numerical simulation of the response of the reinforced concrete retaining wall by performing linear accelerogram analyses using SAP2000/2022 software. The walls of the reinforced concrete retaining wall are modeled by multi-layer shell elements to take into account the non-linear behaviors of the two constituent materials. The effect of stored granular material is taken into account through equivalent masses.

2. Methodology and Tools

2.1. Dynamic Systems Analysis

The finite element method is a valuable tool for modeling and analyzing dynamic systems, offering a combination of flexibility, accuracy, and efficiency for solving complex problems in various scientific and engineering fields [9]. Numerical design offers a powerful and versatile approach for studying the behavior of road loads on reinforced concrete retaining walls. It enables accurate response estimates to be obtained, their behavior to be better understood, and their design to be optimized for improved performance and safety. In a physical model, the formulation of the equations of motion for the modeling of a 1ddl system can be done by Newton's second law, d'Alembert's principle, the principle of virtual work, and Hamilton's principle. Depending on the problem, these principles lead to the same equation of motion. The formulation of the equations of motion for modeling a 1ddl system can be done by Newton's second law, d'Alembert's principle, the principle of virtual work, and Hamilton's principle. Depending on the problem, these principles lead to the same equation of motion [10]-[12]. Whatever the structure considered, it takes the form of a second-order differential equation of the type (**Figure 1**):

$$\ddot{q} + 2 \cdot \xi \cdot w \cdot \dot{q} + w^2 \cdot q = 0 \tag{1}$$

$$M \cdot \ddot{u} + C \cdot \dot{u} + K \cdot u = p(t) \tag{2}$$

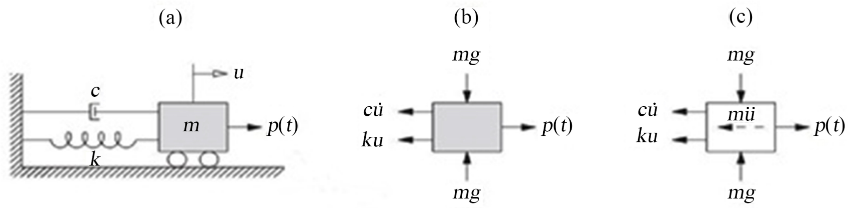

Figure 1. (a) Representation of the mechanical system. (b) External forces. (c) Dynamic force equilibrium diagram.

$\ddot{u}$: Acceleration of motion along *x*.
$\dot{u}$: Speed of motion following *x*.
u: Position of motion following.
M: Mass matrix.
C: Damping matrix.
K: Stiffness matrix.
With

$$w = \sqrt{\frac{k}{m}} \tag{3}$$

$$w = 2 \cdot \pi \cdot f = 2 \cdot \pi \cdot \frac{1}{T} \tag{4}$$

$$\xi = \frac{c}{2 \cdot m \cdot w} = \frac{c}{2 \cdot \sqrt{k \cdot m}} \text{ damping coefficient or degree of damping.} \tag{5}$$

Many researchers have addressed the analysis of road traffic loads on reinforced concrete retaining walls by adopting a source-transmitter-receiver system approach. Notably, An *et al.* 2018 [13], Lee *et al.* 2017 [14], Sun *et al.* (2023) [15], Kim *et al.* 2002 [16], Stacho *et al.* 2022 [17], Seo *et al.* 2019 [18], Wang *et al.* 2022 [19], Qiu *et al.* (2016) [20], Kim *et al.* 2018 [21], Ahac *et al.* 2021 [22], Hajializadeh *et al.* 2015 [23], Liu *et al.* 2019 [24], Khan *et al.* (2023) [25], and Zhang *et al.* 2003 [26]. The use of advanced analysis methods, such as the finite element method, as demonstrated by these authors, enables a deeper understanding of the behavior of reinforced concrete retaining walls and the design of safer, more optimized solutions.

2.2. Rheological Model

The rheological model is a mathematical tool used to describe the behavior of a material under stress [27]. Rheological models are based on the laws of physics and mechanics. They take into account the physical properties of the material, such as viscosity, elasticity, and plasticity [28]. The rheological model applied to each subsystem and to the chosen overall system is elastic-hardening-plastic. The study was divided into four parts, dealing respectively with the truck, wheel-asphalt transfer, asphalt-reinforced concrete retaining wall wave propagation, and the reinforced concrete retaining wall.

2.2.1. Rheological Sub-Model

Truck traffic loads include all the forces exerted by a vehicle on the road surface. These loads can be static or dynamic. Static loads correspond to the vehicle's own weight, uniformly distributed over the wheels. They contribute to the vertical pressure on the pavement and influence the thickness of the road structure layers. Dynamic loads result from vehicle movements and interactions between the wheels and the road surface. These are both horizontal and vertical. Figure 2 shows the rheological state of a truck when subjected to "Yield and damage criterion" [29].

$$\psi = \left(\frac{1}{2} \times E \times \left(\varepsilon - \varepsilon^{p}\right) + \frac{1}{2} \times H \times K^{2}\right) \times (1-d) \tag{6}$$

$d = 1$ completely deteriorated.

From coleman's equation,

$$\sigma = \frac{\partial \psi}{\partial \varepsilon} = E \times \left(\varepsilon - \varepsilon^{p}\right) \tag{7}$$

$$\sigma^{p} = -\frac{\partial \psi}{\partial \varepsilon} \equiv \sigma \tag{8}$$

$$\tilde{\sigma} = \frac{E \times \left(\varepsilon - \varepsilon^{p}\right)}{1-d} \tag{9}$$

where the dissipative stress K associated with K is given as

$$K = \frac{\partial \psi}{\partial K} = -H \times K \tag{10}$$

The yield function is undefined as

$$\phi(\sigma; K) = |\sigma| - \sigma_{Y} - K \tag{11}$$

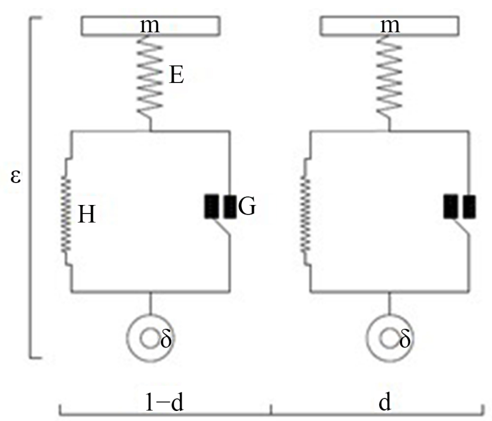

Figure 2. Truck rheology sub-model.

2.2.2. Rheological Sub-Model: Wheel + Asphalt

Figure 3 shows the rheological state of the wheel-asphalt when the material is subjected to the "Yield and damage criterion" [29].

$$\psi = \left(\frac{1}{2}\times E\times\left(\varepsilon-\varepsilon^{p}\right)+\frac{1}{2}\times H\times K^{2}\right)\times\left(1-d\right) \tag{12}$$

$d = 1$ completely deteriorated.

From coleman's equation,

$$\sigma = \frac{\partial\psi}{\partial\varepsilon} = E\times\left(\varepsilon-\varepsilon^{p}\right) \tag{13}$$

$$\sigma^{p} = -\frac{\partial\psi}{\partial\varepsilon} \equiv \sigma \tag{14}$$

$$\tilde{\sigma} = \frac{E\times\left(\varepsilon-\varepsilon^{p}\right)}{1-d} \tag{15}$$

where the dissipative stress K associated with K is given as

$$K = \frac{\partial\psi}{\partial K} = -H\times K \tag{16}$$

The yield function is non defined as

$$\phi\left(\sigma;K\right) = \left|\sigma\right| - \sigma_{Y} - K \tag{17}$$

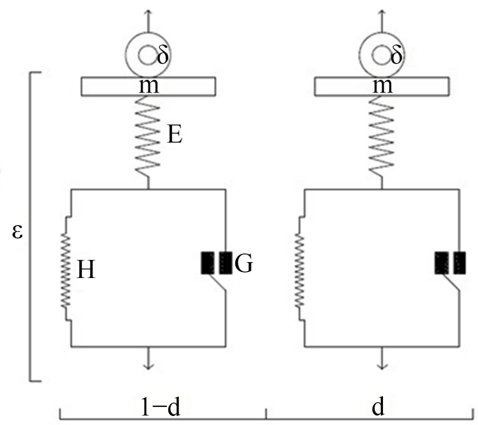

Figure 3. Rheological sub-model truck-asphalt.

2.2.3. Rheological Sub-Model: Asphalt-Reinforced Concrete Retaining Wall

Figure 4 shows the rheological condition of asphalt-reinforced concrete retaining wall when the material undergoes "Yield and damage criterion" [29].

$$\psi = \left(\frac{1}{2}\times E\times\left(\varepsilon-\varepsilon^{p}\right)+\frac{1}{2}\times H\times K^{2}+m\times c^{2}\right)\times\left(1-d\right) \tag{18}$$

$d = 1$ completely deteriorated.

From coleman's equation,

$$\sigma = \frac{\partial\psi}{\partial\varepsilon} = E\times\left(\varepsilon-\varepsilon^{p}\right) \tag{19}$$

$$\sigma^{p} = -\frac{\partial\psi}{\partial\varepsilon} \equiv \sigma \tag{20}$$

$$\sigma^C = \frac{E \times (\varepsilon - \varepsilon^p)}{1-d} \tag{21}$$

where the dissipative stress K associated with K is given as

$$K = \frac{\partial \psi}{\partial K} = -H \times K \tag{22}$$

The yield function is undefined as

$$\phi(\sigma; K) = |\sigma| - \sigma_Y - K \tag{23}$$

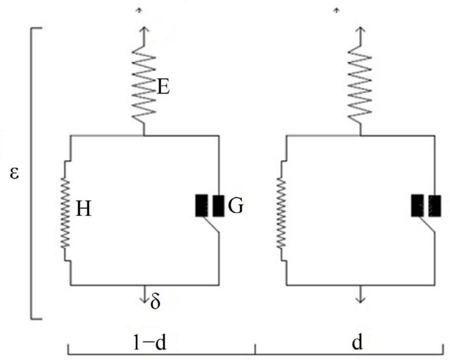

Figure 4. Asphalt rheological sub-model—reinforced concrete retaining wall.

2.2.4. Rheological Model: Reinforced Concrete Retaining Wall

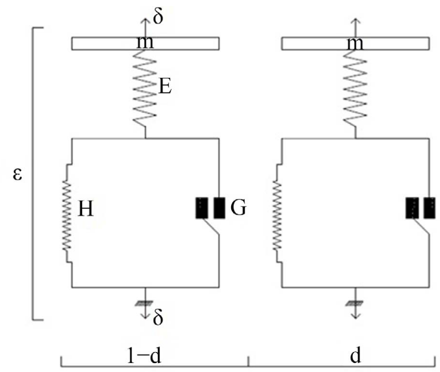

Figure 5. Rheological sub-model for reinforced concrete retaining wall.

Figure 5 shows the rheological state of the reinforced concrete retaining wall when the material undergoes "Yield and damage criterion" [29].

$$\psi = \left(\frac{1}{2} \times E \times (\varepsilon - \varepsilon^p) + \frac{1}{2} \times H \times K^2 + m \times c^2\right) \times (1-d) \tag{24}$$

$d = 1$ completely deteriorated.

From coleman's equation,

$$\sigma = \frac{\partial \psi}{\partial \varepsilon} = E \times (\varepsilon - \varepsilon^p) \tag{25}$$

$$\sigma^p = -\frac{\partial \psi}{\partial \varepsilon} \equiv \sigma \tag{26}$$

$$\sigma^C = \frac{E \times (\varepsilon - \varepsilon^p)}{1 - d} \tag{27}$$

where the dissipative stress K associated with K is given as

$$K = \frac{\partial \psi}{\partial K} = -H \times K \tag{28}$$

The yield function is undefined as

$$\phi(\sigma; K) = |\sigma| - \sigma_Y - K \tag{29}$$

2.2.5. Rheological Model of the System

Figure 6 shows the rheological state of the system as the material undergoes elastic, hardening, and plastic behavior.

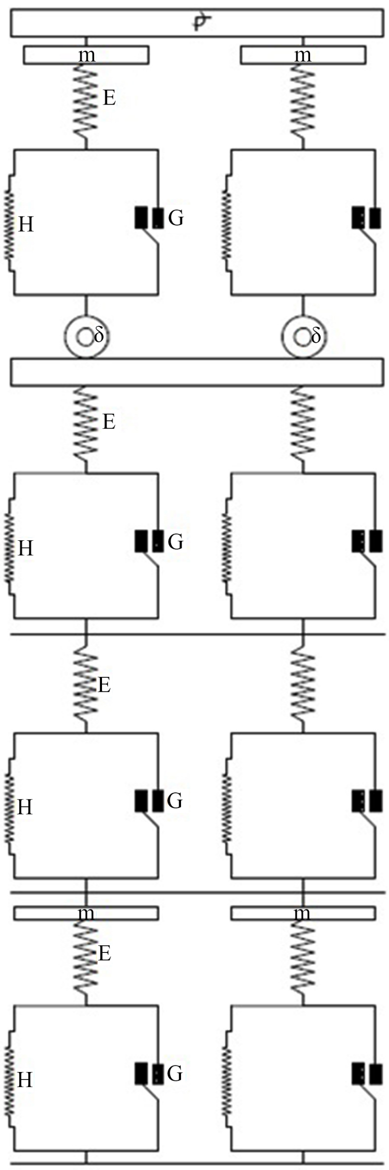

Figure 6. Rheological model of the system.

2.3. Study Environment

2.3.1. Presentation of the Study Area: Dschang-Falaise (Cameroon)

The reinforced concrete retaining wall study will be carried out in the western region, in the town of Dschang, capital of the Menoua department, in the Foréké-Dschang commune. Along the road linking Dschang and Melong, this road has a steep gradient averaging 7.6%. It has a difference in altitude of over 700 m, from the bridge over the Menoua River (713 m), the road reaches an altitude of 1450 m at the summit at the intersection with the road to the Apouh chiefdom, then begins a descent towards the town of Dschang (1350 m). The structure is located at the intersection of latitude 10˚0'33"E and longitude 5˚24'9"N, with an altitude of 1220 m [30] (**Figure 7**).

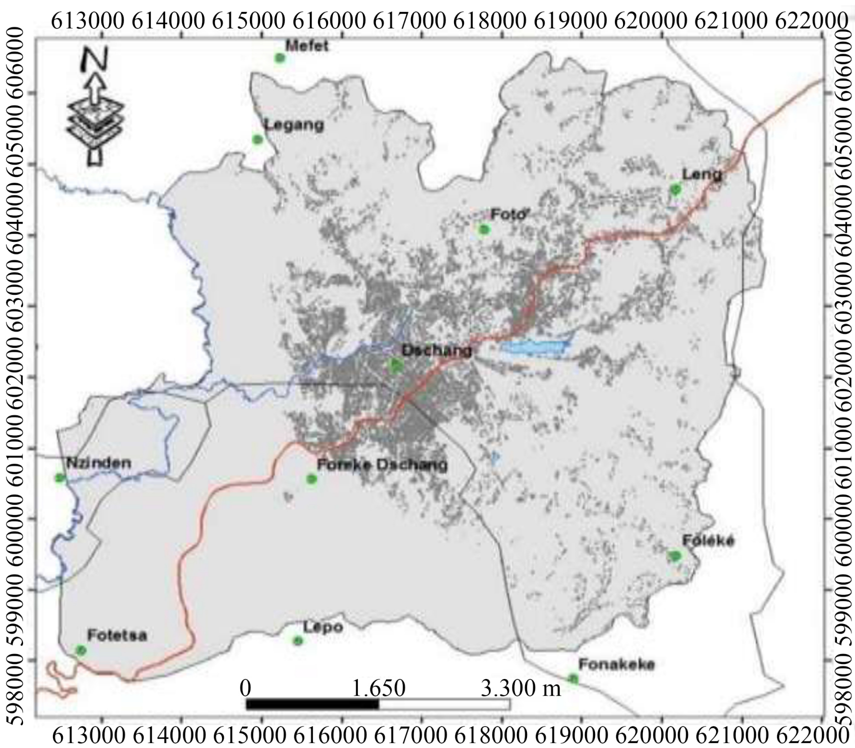

Figure 7. Map of the urban perimeter of Dschang [31].

2.3.2. Geotechnical Aspects of the Site

A. Field work methods [32]

- Material identification: In the field, the touch/smell/wash test, following the methods of, will have to be carried out for the apparent classification of materials and their organic matter composition. The soil is reddish.
- Sampling: At Dschang-Falaise, sampling means taking intact (or undisturbed) samples.

B. Laboratory methods

The characteristics of the soil concerned by this study are its cohesion and the angle of internal friction in the intact state. The tests were carried out at the AB Geotechnical Sarl laboratory in Yaoundé. The aim is to determine certain soil characteristics that are relevant to the forces acting on the reinforced concrete retaining wall. At Dschang-Falaise, tests were carried out on soil samples (foundation and backfill). These included standardized tests such as the water content test, the density test using the water pycnometer method, and the rectilinear shear test using the CASAGRANDE box. The results obtained enabled a comparison to be made between the results obtained in the laboratory and those obtained empirically, in order to adopt the results obtained in the laboratory.

- Moisture content test

Soil samples are taken to determine water content. The procedure followed complies with standard NF P 18555 [33]. For the foundation soil, the water content is 24.44%, and for the retaining soil, it is 21.61%.

- Density test using the water pycnometer method

Density determination by the water pycnometer method is carried out on the soil sample taken. The procedure followed complies with standard NF P 18-555 (1990) [33]. The density of the foundation soil is 2.54, and that of the retaining soil is 2.56.

- Rectilinear shear test with CASAGRANDE box

A quantity of our soil is taken to fill the square plate of the CASAGRANDE apparatus (10 cm square and 3 cm high) [34]. The cohesion and internal angle of friction are 0.10 bar and 7.50 for the foundation soil and 0.15 bar and 7.80 for the retaining soil.

C. Road traffic loads [35]

The road traffic loads considered in this study are:

- Vehicle impact: The impact of a vehicle against the wall can generate large, localized forces.
- Braking and acceleration: Vehicle braking and acceleration forces can create dynamic loads on the reinforced concrete retaining wall.
- Vehicle vibration: Vibrations from moving vehicles can generate dynamic loads on the reinforced concrete retaining wall.

Hence, we have:

- The dynamic load period is the time required for a complete load cycle to occur. It depends on the truck speed and the distance between the truck axles. Assuming a truck speed of 40 km/h and an axle distance of 4 m. We have a period of 0.36 secs.
- The number of load cycles depends on the duration of the analysis and the period of the dynamic loads. Considering an analysis duration of 10 secs, the number of cycles equals 27.78 cycles.
- The dynamic load amplitude is the maximum force applied by the truck to the reinforced concrete retaining wall. It depends on truck weight, truck speed, and road conditions. With a truck weight of 20 tons and poor road conditions, the amplitude is 57142.86 N/m^2.

2.4. Presentation of the Structure's Characteristics

2.4.1. Geometrical Characteristics

Figure 8 shows the configuration of the system studied. The reinforced concrete retaining wall is equipped with a network of barbacanes for rapid drainage of seepage water into the backfill. On the chosen site, we can consider three possible cases for the reinforced concrete retaining wall, depending on our predimensioning assumptions (Table 1 and Table 2).

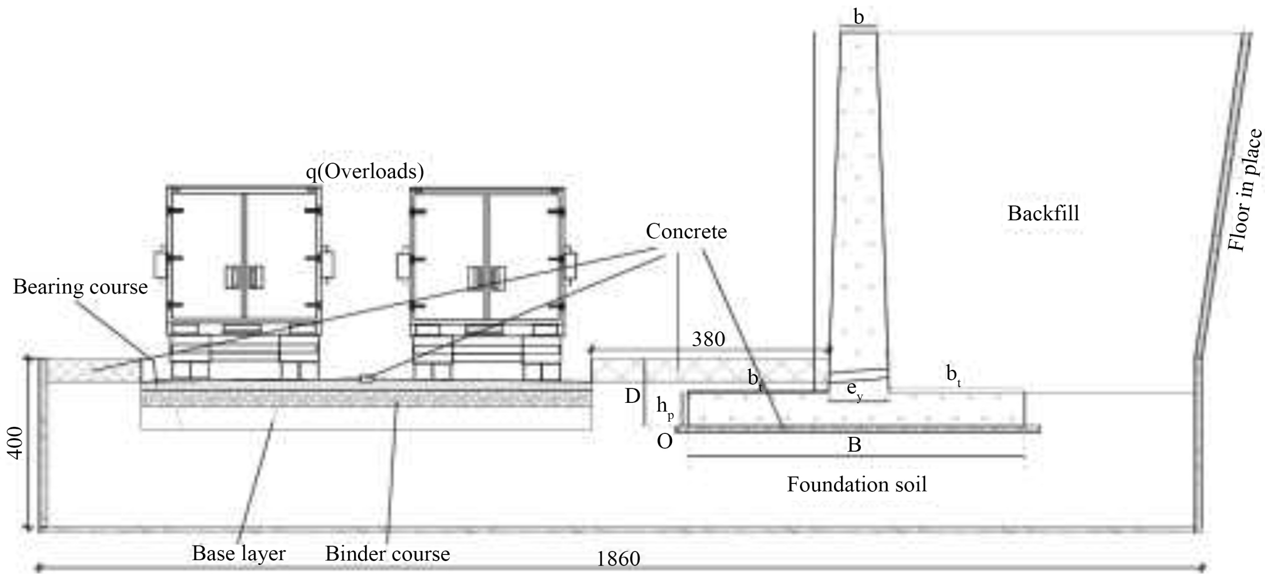

Figure 8. System overview.

Table 1. Retaining wall characteristics.

	Height Wall (H)	Width Sole (B)	Thickness Sole (h_b)	Thickness Bottom Veil (e_v)	Thickness Top Veil (b)	Shoe (b_p)	Heel (b_t)	Mounting Depth (D)
First Case	5.6 m	2.81 m	0.46 m	0.46 m	0.25 m	0.8 m	1.55 m	0.8 m
Second Case	5.6 m	2.81 m	0.46 m	0.51 m	0.30 m	0.8 m	1.55 m	0.8 m
Third Case	5.6 m	2.81 m	0.46 m	0.56 m	0.35 m	0.8 m	1.55 m	0.8 m

Table 2. Material parameters.

	Young's Modulus (MPa)	Fish Coefficient	Weight (KN/m³)	Shear Modulus	Coefficient of Thermal Expansion
Concrete	30,000	0.3	24	11538.462	1.170E−05
Reinforced Concrete Wall	50,000	0.255	24	19920.319	1.170E−05
Foundation Soil	127	0.33	25,4	47.7444	1.170E−05
Backfill Soil	29	0.4	25.6	10.3571	1.170E−05
Bearing Course	4000	0.35	22	1481.4815	1.170E−05
Binder Course	4000	0.35	22	1481.4815	1.170E−05
Base Course	200	0.35	22	74.0741	1.170E−05

2.4.2. Static Characteristics of the Structure

Static design will be carried out in ELU, simultaneously using partial coefficients for actions as indicated in EUROCODE 7 [36].

A. Calculation of the force due to the weight of the concrete wall and footing

- Calculating the force due to the weight of the concrete wall

According to EUROCODE 7 [36], this force is given by the relation

$$W = \delta \times h \times \left(e_v + b\right)/2 \tag{30}$$

where

δ: Specific weight of concrete, *i.e.,* 2500 kg/m^3;

h: Height of the web;

e_v: Bottom veil thickness;

b: Top veil thickness.

- Calculation of the force due to the weight of the footing

According to EUROCODE 7 [36], this force is given by the relation

$$P = \delta \times h_b \times B \tag{31}$$

where

δ: Specific weight of concrete, *i.e.,* 2500 kg/m^3;

h_b: Height of the footing;

B: Width of footing.

- Calculation of thrust

The Coulomb method is used for calculating thrust because it gives satisfactory results in practice for weight walls (rough contact between the reinforced concrete retaining wall and the ground):

δ (Friction angle at wall – soil interface) ≥ 0;

β (Angle of ground surface (fill) to horizontal) ≥ 0;

θ (Angle of rear wall facing with vertical (downstream wall fruit)) ≥ 0.

The thrust coefficients exerted by the backfill on the wall are calculated as follows

φ'_d = 6.253˚; δ_d = 6.253˚; β = 0˚ and θ = 0˚. Thrust coefficient KAγ = 0.746.

B. Model

A 3D reinforced concrete retaining wall, with variable geometries as shown in **Table 1**, was erected 3.80 meters from a road used by vehicles. It is located at Dschang Falaise and supports two carriageways, each 3 meters wide. The earth fills behind the wall has a flat, horizontal surface. The reinforced-concrete retaining wall has a concrete base, with concrete sidewalks on either side. Recessed supports delimit the study area at the bottom, while simple supports are present on the right and left sides.

C. Mesh

The mesh considered is a discretization of the area into objects of maximum size. We have considered quads and triangles only. This finite element model is created using SAP2000. **Figure 9** shows the model considered. The mesh is a 3D finite element discretization with elements along the edge of points 1 to 2 of 0.25 m and along the edge of points 1 to 3 of 0.25 m.

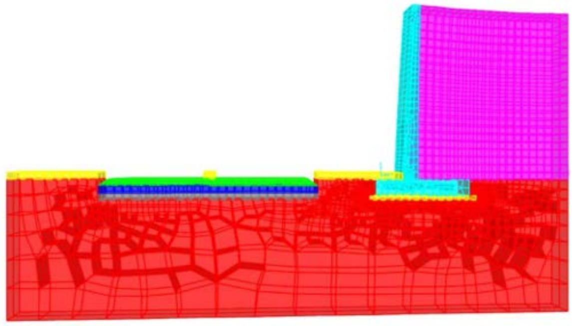

Figure 9. Meshing of the 3 study cases D.

D. Loading

The loads applied are respectively:

- Dead weight;
- Active earth pressure: This is the force exerted by the loose soil backfilled behind the reinforced concrete retaining wall. It is generally distributed in a triangular pattern over the height of the wall, with a maximum value at foot level. The active earth thrust depends on several factors, such as the nature of the soil, the cohesion and angle of internal friction of the soil, the height of the backfill, and the inclination. The joint model considered in SAP2000 is

$$Ax + By + Cz + D = 0 \tag{32}$$

with $D = 106.94656$ KN/m^2 and $C = -19.6$ KN/m^2;

- Passive earth thrust: This is the resisting force exerted by the loose soil in front of the reinforced concrete retaining wall. It has been neglected;
- Loads due to road traffic: These dynamic loads are due to the movement of vehicles on the structure, inducing vibrations and dynamic stresses. Vibratory dynamic loads result from the regular movement of vehicles on the pavement surface. They are generally modeled as cosine loads with frequencies and amplitudes characteristic of the type of traffic and vehicle speed. The load model corresponding to the overload on the pavement is 16.66 KN/m^2, which is the surface pressure load. This overload is the linear modal history with period 0.36 seconds, number of cycles 27.78 cycles, and amplitude 57.14286 KN/m^2.

3. Results and Discussion

3.1. Static Dimensioning

3.1.1. First Case (Figure 10)

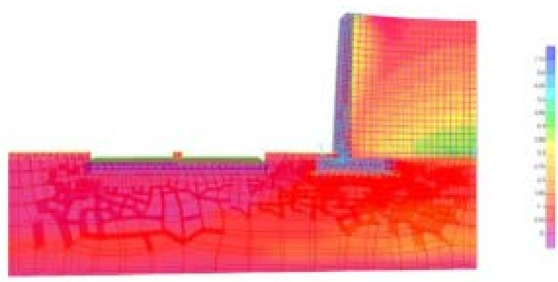

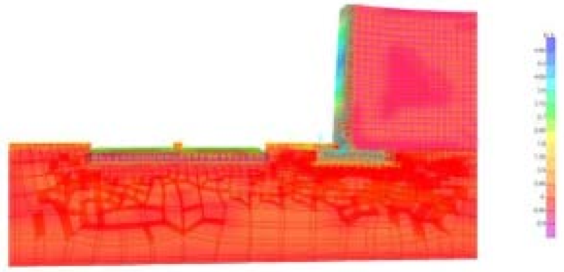

Figure 10. Max strain = 0.007135 MPa and max stress = 4.868798 MPa.

3.1.2. Second Case (Figure 11)

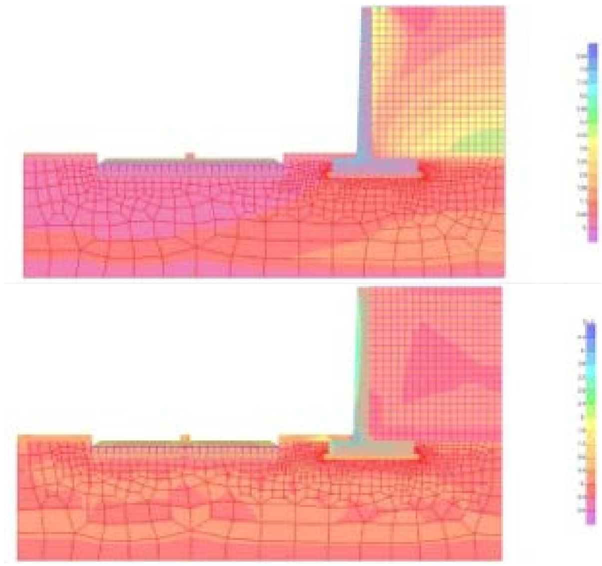

Figure 11. Max strain = 0.008841 MPa and max stress = 4.226914 MPa.

3.1.3. Third Case (Figure 12)

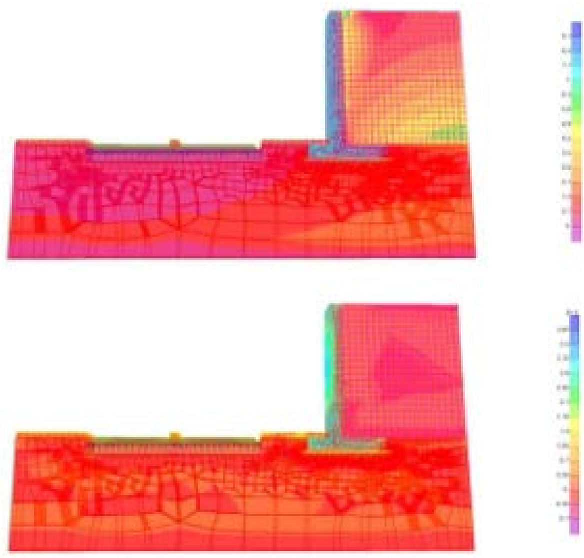

Figure 12. Max strain = 0.009705 MPa and max stress = 3.681698 MPa.

3.2. Spectral Response

Spectral response analysis is a measure of the intensity of the reinforced concrete retaining wall's response to vibratory excitation. It represents the evolution of spectral acceleration as a function of period for a reinforced concrete retaining wall subjected to road traffic loading [37]. The damping coefficient or degree of damping is intrinsically very low and depends on the material of the structure studied. For calculating the response of retaining structures, standard NF EN 1991-2 gives indicative values for the damping coefficient, depending on the material used. The study of road loads was based on the analysis of time history. The cosine function was considered with: Period 0.36 seconds; Number of cycles: 27.78 cycles; Amplitude: 57.14286 KN/m^2.

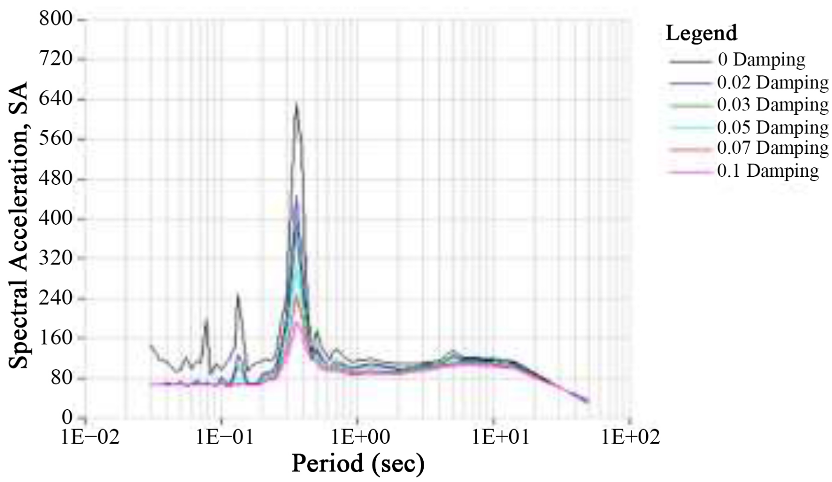

Figure 13. First case: Max (0.357; 633.066002).

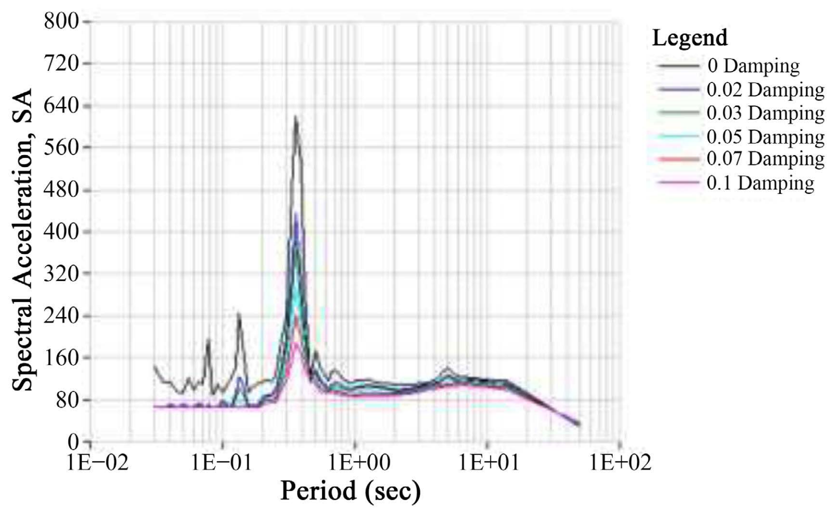

Figure 14. Second case: Max (0.357; 619.669223).

Figures 13-15 show that the spectral acceleration response has a constant period for the gradient or damping coefficient, which varies from 0 to 0.1. As a result, the response of the reinforced concrete retaining wall is greater for short periods (high frequencies) and decreases for long periods (low frequencies). Maximum spectral acceleration values are around 0.12 m/s^2 for a period of 0.05 seconds. This indicates that the retaining wall is susceptible to significant accelerations in this frequency range.

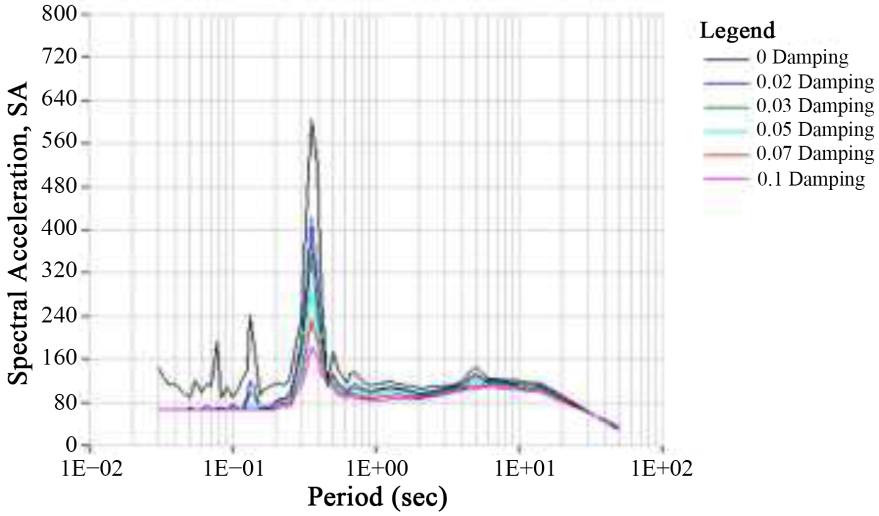

Figure 15. Third case: Max (0.357; 604.12405).

3.3. Dimensioning Road Traffic Loads

Road loads were studied by combining static loads and time history analysis. The analysis considered the period 0.36sec, amplitude 57.14286 KN/m^2, number of cycles 5, and number of steps per cycle 27.78 cycles.

3.3.1. First Case (Figure 16)

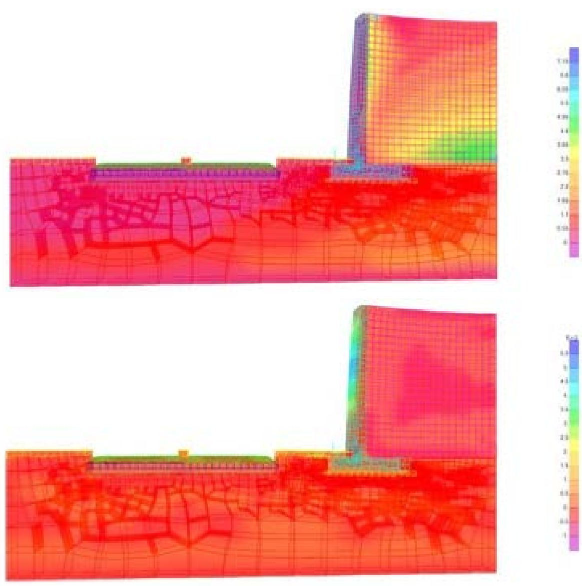

Figure 16. Max strain = 0.007592 MPa and max stress = 5.095827 MPa.

3.3.2. Second Case (Figure 17)

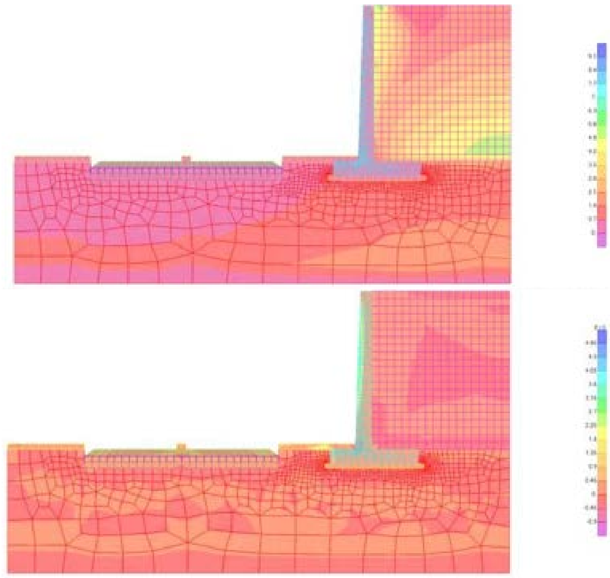

Figure 17. Max strain = 0.009386 MPa and max stress = 4.405626 MPa.

3.3.3. Third Case (Figure 18)

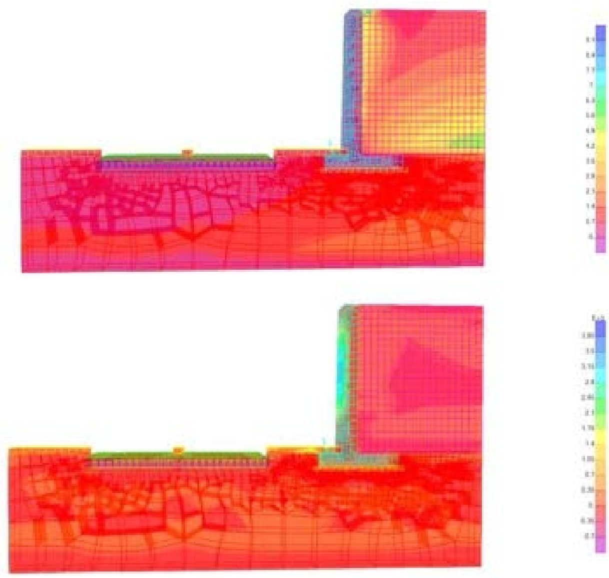

Figure 18. Max strain = 0.009792 MPa and max stress = 3.829364 MPa.

3.4. Assessing the Impact of Traffic Loads

A comparison of the results for the two dimensioning approaches is shown in Table 3.

Based on these values, it can be seen that in both behavioral approaches, the deviation is 6.40% and 4.66%, respectively, for strain and stress in the first case, 6.16% and 4.22%, respectively, for strain and stress in the second case, and 0.89% and 4.01%, respectively, for strain and stress in the third case.

Table 3. Comparison of values for the two design approaches.

	Static Calculation	Traffic Calculation	$\frac{\text{Traffic calculation}}{\text{Static calculation}}$	$\frac{\Delta \text{Calcul}_{\text{Traffic calculation/static}}}{\text{Static calculation}} \times \%$
1ᵉcas, Strain, MPa	0.007135	0.007592	1.064	6.40
1ᵉcas, Stress, MPa	4.868798	5.095827	1.046	4.66
2ᵉcas, Strain, MPa	0.008841	0.009386	1.061	6.16
2ᵉcas, Stress, MPa	4.226914	4.405626	1.042	4.22
3ᵉcas, Strain, MPa	0.009705	0.009792	1.008	0.89
3ᵉcas, Stress, MPa	3.681698	3.829364	1.048	4.01

3.5. Model Potential

It can be seen that the difference between the static and traffic-loaded behavior of stresses and strains decreases with increasing geometry of the reinforced concrete retaining wall when considering the time history analysis. The results are shown in Table 4.

Table 4. Strain and stress results.

	Strain	Stress
First Case	6.40%	4.66%
Second Case	6.16%	4.22%
Third Case	0.89%	4.01%

These results show that dynamic loads caused by road traffic must be systematically incorporated into the design of retaining walls to ensure their safety and durability. For engineers, this means taking dynamic effects into account in design calculations. Furthermore, neglecting these effects can pose risks to the stability of structures. Finally, these findings underscore the need to incorporate traffic-induced vibrations into civil engineering's standard and design codes.

3.6. Model Limitations and Discussions

The model does not take into account the stop, which acts on the safety side. The mechanical properties of the pavement and sidewalk have been taken in general terms, in accordance with current design standards. Natural climatic conditions, corresponding to the exposure environment of these materials, which generally vary, thus inducing certain thermal effects, have not been taken into account.

The study by Otomo *et al.* (2021) [38] on the influence of repeated loading from passing vehicles on the failure of the prefabricated L-type restraint offers promising results. Repeated loading tests on an L-type pseudo-retaining wall revealed that the resistance to failure depends on the applied load magnitude. The greater the load, the fewer repetitions it takes for the rod to break through the backfill soil behind the wall.

4. Conclusions

The results obtained highlight a significant structural response of reinforced concrete retaining walls to dynamic stresses induced by road traffic, challenging the hypothesis of strictly static behavior. The differences observed between static and dynamic analyses, up to 6.40% for deformations and 4.60% for stresses, reflect the significant effects of inertial and dynamic contributions on the overall response of the structure. The spectral analysis also reveals a decreasing trend in the dynamic response as geometric parameters increase, indicating an attenuation effect related to structural rigidity at the structural scale. This behavior suggests a gradual reduction of the dynamic sensitivity with increasing wall dimensions.

Finally, the potential influence of variability in material properties highlights the existence of additional uncertainties that may amplify the response gaps between static and dynamic models. These results confirm the need to explicitly integrate the dynamic effects of traffic into design approaches in order to improve the robustness and reliability of support structures.

Data Availability

The authors confirm that the data supporting the results of this study, obtained at the laboratory Geotechnical Sarl in Yaoundé, are available in the article and/or in its supplementary materials.

Funding

Cameroonian Government.

Conflicts of Interest

The authors declare no conflicts of interest regarding the publication of this paper.

References

[1] Kumagai, H., Kono, T. and Aoki, M. (2023) Evaluation of the Behavior of Retaining Walls and Surrounding Ground by Finite Element Method Analysis. In: *Lecture Notes in Civil Engineering*, Springer, 330-337. https://doi.org/10.1007/978-3-031-12851-6_40

[2] Shin, J.W. and Kim, D.S. (2004) Comparison of Displacement of the Braced Retaining Wall by Developed Elasto-Plastic Analysis. *Journal of the Korean Society of Safety*, **19**, 112-118.

[3] Sheth, A.K. and Raghavani, R. (2021) Comparison of Conventional Method with Finite Element Analysis Using Plaxis 2D for Cantilever and Anchored Sheet Pile Walls. In: *Lecture Notes in Civil Engineering*, Springer, 577-583. https://doi.org/10.1007/978-981-33-6466-0_53

[4] Liu, Y., Yao, Z.Y., Shao, M.X., Liu, H.Z. and Zhao, Y.L. (2021) Mechanical Behavior of the Reinforced Retaining Wall under Vehicle Load. *Mathematical Problems in En-*

gineering, **2021**, 1-15. https://doi.org/10.1155/2021/2197572

[5] Geng, M. (2021) A Short Review on the Dynamic Characteristics of Geogrid-Reinforced Soil Retaining Walls under Cyclic Loading. *Advances in Materials Science and Engineering*, **2021**, Article ID 5537912. https://doi.org/10.1155/2021/5537912

[6] Liu, Z., Shi, K., Huang, T., *et al.* (2017) Field Test of Static and Dynamic Response of Reinforced Earth Retaining Wall under Vehicle Load. *Hydrogeology and Engineering Geology*, **44**, 91-97.

[7] Liu, Z., He, F., Huang, T.Q. and Jiang, M.D. (2019) Additional Earth Pressure of Retaining Wall Caused by Vehicle Load. *Journal of Highway and Transportation Research and Development* (*English Edition*), **13**, 16-23. https://doi.org/10.1061/jhtrcq.0000663

[8] Sahibbi, A., Hazarika, H. and Ishibashi, I. (2024) Effect of Surcharge Load on the Magnitude and Distribution of Lateral Earth Pressure against Rigid Retaining Wall. *Japanese Society of Civil Engineering West Branch*, Chuo-ku, 8 March 2025.

[9] Rousseau, J. (2009) Numerical Modeling of the Dynamic Behavior of Structures under Severe Impact with a Discrete Element/Finite Element Coupling... Sciences de l'ingénieur [Physics]. Université Joseph-Fourier-Grenoble I.

[10] Lestuzzi, P. and Smith, I.F.C. (2023) Structural Dynamics. Bases and Applications for Civil Engineering. 3rd Edition, Presses Polytechnique's and Universitaires Romandes.

[11] Chatzigogos, C.T., Pecker, A. and Salençon, J. (2009) Macroelement Modeling of Shallow Foundations. *Soil Dynamics and Earthquake Engineering*, **29**, 765-781. https://doi.org/10.1016/j.soildyn.2008.08.009

[12] Drapie, S. (2016) Dynamique des Solides et des Structures. 5ieme édition, Département Mécanique et Procèdes d'Elaboration, Centre Science des Matériaux et des Structures & UMR CNRS 5146 et Ecole Nationale Supérieure des Mines de Saint-Etienne.

[13] An, Y., Leo, C., Liyanapathirana, S. and Wong, H. (2018) Vehicular Impact Loading on the Barrier of a Retaining Wall System and Its Effect on the System Foundation. In: *Proceedings of GeoShanghai* 2018 *International Conference*: *Transportation Geotechnics and Pavement Engineering*, Springer, 199-206. https://doi.org/10.1007/978-981-13-0011-0_22

[14] Lee, K., Lim, D. and Chung, M.K. (2017) Analysis of Lateral Earth Pressures on Retaining Wall from Traffic Load Distribution. *Journal of the Korean Geosynthetics Society*, **16**, 43-55.

[15] Sun, X., Liu, W., Zhai, H., Ding, D. and Guo, J. (2006) Vibration Effects of Metro Trains on Sensitive Instruments and the Study of the Mitigation Measures. *Tunnelling and Underground Space Technology*, **21**, 299. https://doi.org/10.1016/j.tust.2005.12.156

[16] Kim, J.S. and Barker, R.M. (2002) Effect of Live Load Surcharge on Retaining Walls and Abutments. *Journal of Geotechnical and Geoenvironmental Engineering*, **128**, 803-813. https://doi.org/10.1061/(asce)1090-0241(2002)128:10(803)

[17] Stacho, J. and Sulovska, M. (2022) Analysis of Static and Cyclic Traffic Loading of an Embankment Supported by a Geogrid Retaining Structure. *Slovak Journal of Civil Engineering*, **30**, 1-8. https://doi.org/10.2478/sjce-2022-0015

[18] Seo, S., Jin, H. and Chung, M. (2019) Assessment of Equivalent Heights of Soil for the Lateral Earth Pressure against Retaining Walls Due to Design Truck Load by 3D Numerical Analysis. *Journal of the Korean Geosynthetics Society*, **18**, 75-85.

[19] Wang, H., Wang, N., Yang, G. and Ma, J. (2022) Model Test and Numerical Simulation

Research of Reinforced Soil Retaining Walls under Cyclic Loads. *Sustainability*, **14**, Article 15643. https://doi.org/10.3390/su142315643

[20] Qiu, H.Z., Kong, J.M. and Wang, R.C. (2016) Dynamic Active Earth Pressures of the Retaining Piles with Anchors under Vehicle Loads. *Shock and Vibration*, **2016**, 1-8. https://doi.org/10.1155/2016/4023827

[21] Kim, D., Jin, H., Seo, S., Park, J., *et al.* (2018) Assessment of Equivalent Heights of Soil for the Lateral Earth Pressure against Retaining Walls Due to Design Truck Load. *Journal of the Korean Geosynthetics Society*, **17**, 119-128. https://doi.org/10.12814/jkgss.2018.17.4.119

[22] Ahac, M., Ahac, S. and Lakušić, S. (2021) Long-Term Sustainability Approach in Road Traffic Noise Wall Design. *Sustainability*, **13**, Article 536. https://doi.org/10.3390/su13020536

[23] Hajializadeh, D., Stewart, M.G., Enright, B. and O'Brien, E. (2015) Spatial Time-Dependent Reliability Analysis of Reinforced Concrete Slab Bridges Subject to Realistic Traffic Loading. *Structure and Infrastructure Engineering*, **12**, 1137-1152. https://doi.org/10.1080/15732479.2015.1086385

[24] Liu, Y., Yao, Z., Shao, M., Liu, H. and Zhao, Y. (2021) Mechanical Behavior of the Reinforced Retaining Wall under Vehicle Load. *Mathematical Problems in Engineering*, **2021**, Article ID 2197572. https://doi.org/10.1155/2021/2197572

[25] Khan, S.A., Karray, M. and Paultre, P. (2024) Seismic Behavior of Retaining Walls: A Critical Review of Analytical and Field Performance Studies. *Geotechnics*, **4**, 54-77. https://doi.org/10.3390/geotechnics4010004

[26] Zhang, Y.P., Gao, Y.T., Fang, Z.L., *et al.* (2003) Instability Analysis of Retaining Walls under Random Vehicle Loading Condition. *Chinese Journal of Engineering*, **25**, 18-22. (In Chinese)

[27] Pulatsu, B., Kim, S., Erdogmus, E. and Lourenço, P.B. (2020) Advanced Analysis of Masonry Retaining Walls Using Mixed Discrete-Continuum Approach. *ICE Proceedings Geotechnical Engineering*, **174**, 302-314.

[28] Feba, S.T. and Kuriakose, B. (2016) Nonlinear Finite Element Analysis of Unreinforced Masonry Walls. *Applied Mechanics and Materials*, **857**, 142-147. https://doi.org/10.4028/www.scientific.net/amm.857.142

[29] Rao, S.S. (2004) Engineering Optimization Theory and Practice. 4th Edition, New Age International Ltd.

[30] Temgoua, E., Tsafack, H.N., Pfeifer, H.-R. and Njine, T. (2015) Levels of Major Elements and Trace Elements in Soil and Some Vegetables from the Town of Dschang, Cameroon. *African Crop Science Journal*, **23**, 35-44.

[31] Kamgne Kamwa, L.P. and Tsalefac, M. (2020) Processus d'intégration des migrants Mbororo à l'économie urbaine: Cas de Bafoussam et Dschang (Ouest-Cameroun). *European Scientific Journal*, **16**, 155. https://doi.org/10.19044/esj.2020.v16n17p155

[32] Houben, H., Rigassi, V. and Garnier, P.H. (1996) Compressed Earth Blocks: Production Equipment, CRATerre, Brussels, Belgium, 149 p.

[33] AFNOR (1990) NF P 18-555 Aggregates. Measurement of Densities, Absorption Coefficient and Water Content of Fine Aggregates.

[34] AFNOR (1994) NF P94-071-1 Soil Investigation and Testing. Direct Shear Test with Shearbox Apparatus. Part 1: Direct Shear.

[35] Ndibi, E.D.D., Mbossi, E.F., Wokwenmendam, N.P., *et al.* (2021) Probabilistic Seismic Hazard Assessment for the Main Cities along the Continental Section of the Cameroon Volcanic Line. *Arabian Journal of Geosciences*, **14**, Article No. 796.

[36] AFNOR (2005) NF EN 1997-1 Eurocode 7: Geotechnical Design, Part 1: General Rules.

[37] Guillard, Y. (2017) Transmission of Vibrations Caused by Road Traffic, Regional Civil Engineering Laboratories, Strasbourg; EDP Sciences.

[38] Otomo, Y. and Maruyama, O. (2021) Influence of Repeated Load of Passing Vehicle on Failure of Precast L-Type Retaining Wall. *Journal of Japan Society of Civil Engineers*, *Series C* (*Geosphere Engineering*), **77**, 248-257. https://doi.org/10.2208/jscejge.77.3_248